www.elsevier.com/locate/memsci

Rejection of disinfection by-products by RO and NF membranes: Influence of solute properties and operational parameters

Katrin Doederer, Maria José Farré, Marc Pidou, Howard S. Weinberg, Wolfgang Gernjak

PII: S0376-7388(14)00405-0
DOI: http://dx.doi.org/10.1016/j.memsci.2014.05.029
Reference: MEMSCI12937

To appear in: *Journal of Membrane Science*

Received date: 11 December 2013
Revised date: 9 May 2014
Accepted date: 17 May 2014

Cite this article as: Katrin Doederer, Maria José Farré, Marc Pidou, Howard S. Weinberg, Wolfgang Gernjak, Rejection of disinfection by-products by RO and NF membranes: Influence of solute properties and operational parameters, *Journal of Membrane Science,* http://dx.doi.org/10.1016/j.memsci.2014.05.029

Rejection of disinfection by-products by RO and NF membranes: Influence of solute properties and operational parameters

Katrin Doederer[1], Maria José Farré[1], Marc Pidou[1,#], Howard S. Weinberg[2] and Wolfgang Gernjak[1] *

[1]The University of Queensland, Advanced Water Management Centre, Level 4 Gehrmann Building (60), 4072 St Lucia, Brisbane, QLD, Australia

[2]University of North Carolina, Gillings School of Global Public Health, Department of Environmental Sciences and Engineering, Michael Hooker Research Center, Chapel Hill, NC 27599-7431, USA

* Corresponding author: Dr Wolfgang Gernjak, Email: w.gernjak@awmc.uq.edu.au, Ph +61-7-33463219

[#] Present address: Cranfield University, Environmental Science and Technology Department, School of Applied Sciences, Cranfield, MK43 0AL, UK

Abstract (100-200words)

The objective of this study was to determine the influence of solute properties and operational parameters on disinfection by-product (DBP) rejection by reverse osmosis (RO) and nanofiltration (NF) membranes. This was achieved by assessing the removal efficiency for 29 DBPs likely to be formed during disinfection of secondary effluents. The DBPs investigated were trihalomethanes, iodinated-trihalomethanes, haloacetonitriles, chloral hydrate, haloketones, halonitromethanes and haloacetamides.

The performance of an NF and a low pressure RO membrane was investigated within a range of different pHs, temperatures, transmembrane fluxes, crossflow velocities and ionic strengths. Rejection decreased significantly with increasing temperature and decreasing transmembrane flux, while the influence of the other operational parameters was minimal with a few exceptions detailed in the manuscript.

Multiple linear regression was used to determine the physico-chemical solute properties contributing significantly to DBP rejection. For NF, geometric parameters were revealed to be the dominant molecular descriptors influencing rejection, whereas for RO, besides size exclusion, solute-membrane interaction played an important role. A predictive model based on multiple linear regression was established that could forecast rejection of DBPs as a function of membrane operation parameters and DBP properties.

Keywords:

reverse osmosis; nanofiltration; disinfection by-products; modelling; multiple linear regression; operational parameters

Abbreviations

BCAcAm	Bromochloroacetamide
BCAN	Bromochloroacetonitrile
BCIM	Bromochloroiodomethane
BDCAcAm	Bromodichloroacetamide
BDCM	Bromodichloromethane
BDIM	Bromodiiodomethane
BIAcAm	Bromoiodoacetamide
CDIM	Chlorodiiodomethane
CH	Chloral hydrate
CIAcAm	Chloroiodoacetamide
DBAcAm	Dibromoacetamide
DBAN	Dibromoacetonitrile
DBCAcAm	Dibromochloroacetamide
DBCM	Dibromochloromethane
DBIM	Dibromoiodomethane
DBP	Disinfection by-product
DCAcAm	Dichloroacetamide
DCAN	Dichloroacetonitrile
DCIM	Dichloroiodomethane
DHAN	Dihalogenated acetonitriles
DIAcAm	Diiodoacetamide
DM	Dipole moment
GC-ECD	Gas chromatograph with electron capture detector
HAA	Haloacetic acids
HAcAm	Haloacetamides
HAN	Haloacetonitriles

HK	Haloketones
HNM	Halonitromethanes
I-THM	Iodinated trihalomethanes
MLR	Multiple linear regression
MV	Molecular volume
MW	Molecular weight
NDMA	N-nitrosodimethylamine
NF	Nanofiltration
PSA	Polar surface area
RO	Reverse osmosis
TBAcAm	Tribromoacetamide
TBM	Tribromomethane
TBNM	Tribromonitromethane
TCAcAm	Trichloroacetamide
TCAN	Trichloroacetonitrile
TCM	Trichloromethane
TCNM	Trichloronitromethane
THM4	Sum of trihalomethanes (TCM, BDCM, DBCM, TBM)
TIM	Triiodomethane
VIF	Variance inflation factor
1,1-DCP	1,1-Dichloropropanone
1,1,1-TCP	1,1,1-Trichloropropanone

1. Introduction

With increased water demand and decreased availability of traditional water sources, pressure driven membrane processes such as nanofiltration (NF) and reverse osmosis (RO) have become an important alternative water treatment technology to augment water supplies with water produced from alternative sources [1]. In particular, integrated membrane systems using low pressure membranes such as ultra/micro filtration followed by RO/NF membranes have developed to an industrial standard for potable reuse applications [2], due to their high treatment efficiency for the removal of salts, metals, endocrine disrupting compounds, pharmaceuticals, personal care products and other emerging contaminants [3]. However, a major limitation for RO/NF membrane performance is membrane fouling. Four types of fouling can occur including inorganic (scaling), particulate, organic and biological. It has been shown that fouling has adverse effects on membrane operation such as an increase in pressure drop, decrease in salt rejection and flux decline [4]. To specifically limit biofouling, the water is generally disinfected with chemical agents, such as chlorine or chloramines [4,5]. However, as an unintentional consequence of this treatment, disinfection by-products (DBPs) are formed by the reaction between organic and inorganic matter and disinfectants. DBPs in drinking water have been found to pose potential public health risks [6,7] through routes of ingestion, inhalation and dermal adsorption. Therefore, the control of those compounds in water treatment systems for direct or indirect potable reuse applications is regulated in many countries. In addition to trihalomethanes (THMs) and haloacetic acids (HAAs), other emerging DBPs including haloacetonitriles (HANs), haloketones (HKs) and halonitromethanes (HNMs) have been detected after chlorination and chloramination of surface waters [6] and secondary effluents [8,9].

The removal of trace organic contaminants by RO and NF membranes has been studied quite extensively, with studies assessing the impact of molecular properties [10,11] and membrane operations, such as feed pressure, transmembrane flux, crossflow velocity, ionic strength and pH [12-18]. Research on small organic solutes in general and DBPs in particular however is very limited with only a small number of studies looking at either THMs, HAAs, HANs or N-nitrosamines [16-26]. Rejection of N-nitrosodimethylamine (NDMA) by RO membranes has been reported to be between 10 and 40% [27,28] whereas rejections of above 50% have been found for HANs [23,26]. On the other hand, removal efficiencies of HAAs have been reported above 90% [20,24] and THM rejections have generally been reported above 60% [22,25]. Among these different published studies, operational factors and solute properties

have only been reported for N-nitrosamines in the studies by Fujioka *et al.* [18] and Steinle-Darling *et al.* [28]. These authors observed that an increase in pH and ionic strength led to a minor impact only on the smaller N-nitrosamines, while increasing temperature caused a significant drop in rejection for all the N-nitrosamines studied [18]. It was concluded that N-nitrosamine removal is mainly governed by size exclusion [18].

Due to their physico-chemical properties, DBPs may not be removed very well by membranes. In fact, previous work showed that trace organic solutes can adsorb on the membrane and diffuse through the membrane matrix to reach the permeate side [10]. Other mechanisms besides adsorption, including size exclusion and electrostatic repulsion, have been identified [11,12]. Those rejection mechanisms are not only governed by solute and membrane properties but also by operational conditions and feed water quality [13]. For a deeper understanding of the DBP rejection mechanisms it is important to identify the factors controlling the permeation process that may change during full-scale application. For instance, the feed solution temperature can change due to seasonal variation and increase up to 30˚C in summer in Australia while in Asia and Africa it might be even higher [29]. Across the pressure vessels in full scale installations, the crossflow velocity decreases and the ionic strength increases. In fact, ionic strength has been found to influence organic solute rejection by NF [12,30]. Additionally, the pH of the feed water is generally adjusted in the range of pH 6 to 8 prior to filtration [31]. On the other hand, DBP concentrations were found to be relatively stable during HQRW production [32] and a change in THM concentration from 20 to 200 µg/L influenced rejection by less than approximately 15% by two NF membranes at 10 bar [33].

In the context of using reclaimed water to overcome present and future challenges to water supply provision in arid areas DBPs are an important class of organic compounds. Complying with DBP regulations is already among the most challenging water quality requirements for recycled water providers using treatment trains based on reverse osmosis [34]. This is due to the necessity of applying disinfectants for biofouling control of reverse osmosis membranes and the abundance of DBP precursors in secondary effluent. In particular, precursors of nitrogen containing DBPs, which are of higher health concern than their carbon based analogues, are abundant in secondary effluent [9]. As described above, the required continuous disinfection results in the formation of a variety of different DBPs with a wide range of intrinsic properties during the disinfection of the secondary effluents upstream of RO filtration [8]. One goal of this study was to investigate the DBP removal by both RO and

NF membranes using a great mixture of commonly occurring DBPs, including four THMs, six I-THMs, two HKs, four HANs, two HNMs, chloral hydrate (CH) and ten HAcAms. In addition, this work aimed to elucidate the influence of operational and feed solution parameters on DBP rejection by both RO and NF membranes and the impact of pH, ionic strength, permeate flux, crossflow velocity and temperature was examined and discussed. The third goal of the manuscript was to apply multiple linear regression to a generated dataset to allow the comparison of the importance of each influencing parameter. Furthermore, a model predicting rejection based on molecular properties and membrane operation conditions was developed and validated.

2. Materials and methods

2.1 Chemicals

For this study 4 trihalomethanes (THM), 6 iodinated trihalomethanes (I-THM), 4 haloacetonitriles (HAN), chloral hydrate (CH), 2 halonitromethanes (HNM), 2 haloketones (HK) and 10 haloacetamides (HAcAm) were chosen within a wide range of molecular properties (Table 1). The groups of THMs, I-THMs, HANs, HNMs and HKs do not possess ionisable functional groups. Consequently, in aqueous solution they were present as neutral solutes. The acid dissociation constants (pKa) of the ionizable compounds, including CH and the HAcAms, ranged from 9.5 to 11.2 (ChemAxon) which indicates that they were not negatively charged in the pH range studied (pH 4.5 to 8.5). Electrostatic repulsion is only expected to play a role at baseline conditions (pH 6.8) for TCAcAm due to a calculated pKa value of 7.3.

THMs, CH, dichloro- and trichloroacetamide were purchased from Sigma-Aldrich (Castle Hill, Australia), as a mix prepared in methanol at 5000 µg/mL for each substance. HANs and HKs were purchased as an EPA 551B Halogenated Volatiles Mix at 2000 µg/mL each in acetone (Sigma-Aldrich). HNMs, I-THMs and the remaining HAcAm standards were purchased at between 90 and 95% purity from Orchid Cellmark (New Westminster, BC, Canada). The 6 I-THMs were prepared at 1500 µg/mL in methanol while the 10 HAcAms mix and TBNM were each prepared in methyl tertiary butyl ether (MtBE) at 5000 µg/mL. 1,2-dibromopropane (97% Sigma-Aldrich) was used as internal standard. Analytical grade 99.9% Chromasolv® MtBE was purchased from Sigma-Aldrich and used, in addition to solution preparation, as extraction solvent. Anhydrous sodium sulphate (10-60 mesh) was purchased from Mallinckrodt chemicals (Phillipsburg, USA). For pH adjustment, hydrochloric acid and sodium hydroxide were used. Univar® analytical reagents NaCl and KH_2PO_4 were purchased from Ajax Finechem Pty Ltd. All aqueous solutions were prepared in Milli-Q water.

2.2 DBP Analysis

Permeate samples were collected in 60mL glass vials sealed with a cap containing a Teflon-lined septa and kept on ice for the duration of the sampling (i.e., 15 minutes for baseline conditions and up to 45 minutes for the lowest flux experiments). In order to minimize volatilisation during the extended sample collection, the septum was pierced with an 0.8 mm vent so that the displacement of air from the vial could occur meanwhile a second port

allowed for sample collection. A control sample of Milli-Q water spiked with 50 µg/L of THMs, CH, HAcAms, HANs, HNMs, and 20 µg/L of the I-THMs in the same type of vial was adjusted to the same pH as the samples and accompanied all samples in order to determine any losses during sample handling due to volatilisation. No losses were observed for the duration of the permeate sampling, ensuring also that no decrease of DBP concentration by hydrolysis occurred. Immediately after sample collection, duplicate 30 mL aliquots were pH-adjusted to 3.5 using 0.2 M sulphuric acid and liquid–liquid extracted with 3 mL methyl tert-butyl ether (MtBE) (containing 100 µg/L internal standard) in the presence of 10 g of pre-baked (at 500°C) sodium sulphate. Samples were vortexed for 1 minute. After settling for 5 minutes, 1.5 mL of the MtBE layer was transferred to gas chromatography (GC) vials for separate injection onto two different columns (DB1 and DB5) and for parallel double pulsed splitless injection (200ºC) on an Agilent 7890A gas chromatograph with ^{63}Ni electron capture detector (GC-ECD). Chromatographic separation of the DBPs was performed using a DB-5 column (30 m x 0.25 mm i.d., 1.0 µm film thickness, Agilent), while a DB-1 column (30 m x 0.25 mm i.d., 1.0 µm film thickness, Agilent) was used for confirmation. The oven temperature program was 35°C for 25 min, ramped to 100°C at 2°C/min and held for 2 minutes, then ramped to 200ºC at 5°C/min, and final ramp at 50°C/min to 280°C leading to a total run time of 81.1 minutes. The extraction and analysis procedures for DBPs were adapted from Weinberg *et al.* [35]. This long run allows for analysis of all the targeted DBPs from a single injection. The reporting limit for the HAcAms was 0.5 µg/L and 0.1 µg/L for all other DBPs.

2.3 Filtration tests

2.3.1 Membranes

One RO (ESPA2, Hydranautics, Oceanside, CA, USA) and one NF (NF90, Dow Filmtec, Minneapolis, MN, USA) membrane were used in this study. The ESPA2 is a low pressure RO membrane commonly used in water reuse applications [36] while the NF90 is a tight NF membrane used in softening and brackish water treatment applications [37]. The membrane coupons used for the filtration experimentts were cut from unused 4 inch modules in both cases. The active surface layer of both membranes is made of a polyamide thin film composite. Inherent characteristics of both membranes can be found in the Supporting Information (SI) (Table SI-1).

2.3.2 Bench-scale filtration system

Experiments in this study were carried out on a flat sheet cross-flow system (Figure 1).

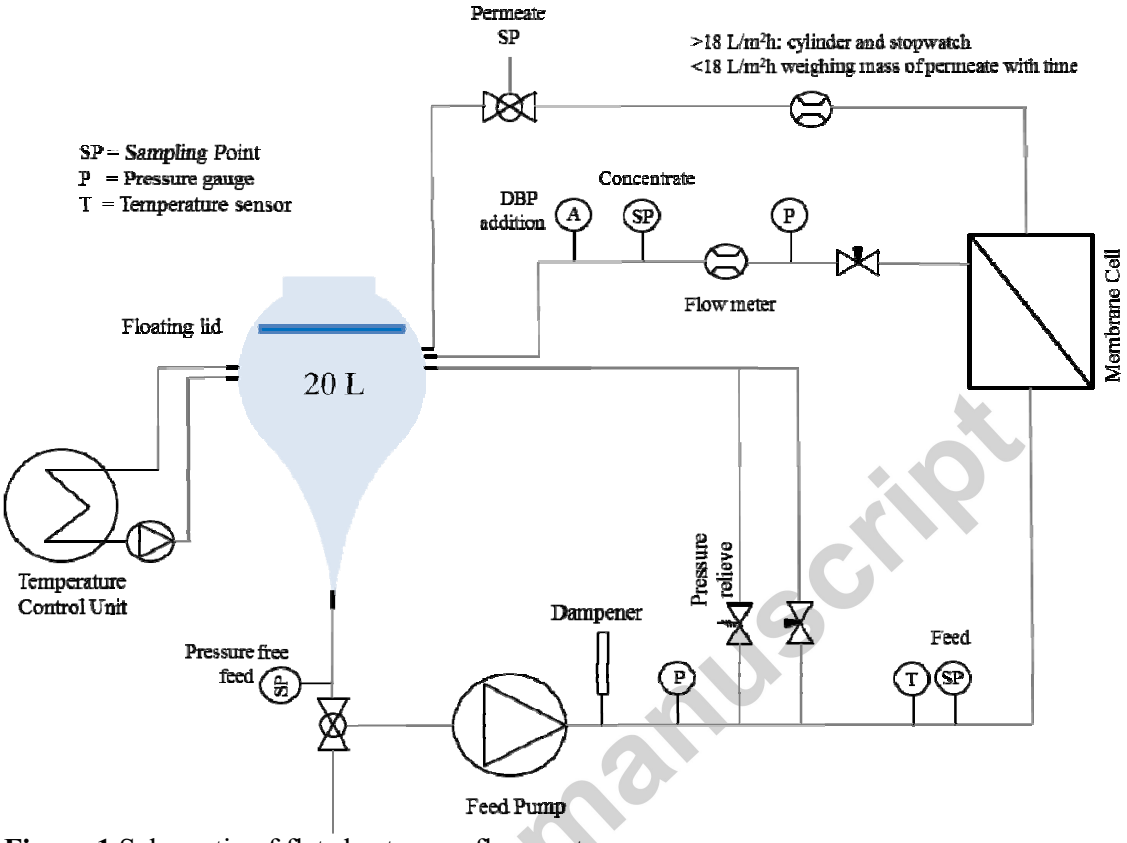

Figure 1 Schematic of flat sheet cross-flow system

To minimize adsorption losses of the DBPs, all system components in contact with the water were built of stainless steel, glass or Teflon. The 20 L feed reservoir was made of clear glass while the plumbed tubing and membrane cell used stainless steel. The membrane cell has an effective membrane area of 139 cm^2 and a feed channel height of 1.6 mm. A floating lid made of Teflon and placed in the reservoir on top of the liquid was used to reduce volatilisation losses. A crossflow velocity of 0.12 m/s was selected to simulate conditions at full-scale treatment plants. This value is an average of crossflow velocities across a single stage at three advanced water treatment plants in south east Queensland during normal operation. This represents a low cross-flow velocity where the concentration polarisation can influence the solute rejection. Permeate flow was measured with a cylinder and stopwatch for permeate fluxes >18 L/m^2h while the lower permeate fluxes were determined by weighing the mass of permeate per unit of time. The concentrate flow was controlled by a rotameter (Vögtlin Instruments AG, Switzerland). Feed pressure was monitored with an analogue pressure gauge (Ashcroft, Stratford, CT, USA) and controlled with a back pressure needle valve (Swagelok, Melbourne, Australia) in the concentrate line. Temperature control and

mixing was achieved by recirculating the feed solution through a stainless steel coil immersed in a temperature controlled bath (Lauda Alpha, Lauda-Königshofen, Germany). To avoid photodegradation losses of the I-THMs, the feed reservoir was protected from light.

2.3.3 Experimental protocols

Prior to each experiment the selected membrane coupon was rinsed thoroughly with Milli-Q water. To ensure a stable permeate flux, the membrane coupon was compacted overnight at 11 bar using Milli-Q water. When measuring the pure water permeability, the transmembrane pressure was reduced to 3.5 bar and 1.5 bar after compaction for the ESPA2 and NF90, respectively, to reach a flux of about 18 L/m^{2}h. Salt rejection was determined using a 1,500 mg/L NaCl solution at 7.5 bar for the ESPA2 and a 2,000 mg/L Mg_2SO_4 at 4.8 bar for the NF90. Membrane coupons were used in the DBP study after achieving a minimum salt rejection of 98.5% for the ESPA2 and 97% for the NF90. After rinsing the system thoroughly, the Milli-Q water was replaced with 14 L of background electrolyte solution consisting of 7 mM NaCl and 1 mM KH_2PO_4. The latter was chosen to be able to maintain a pH at 6.8 over a minimum duration of 2 weeks while the former was used to obtain a conductivity of around 900 µS/cm which is typical for a secondary effluent [38]. Unless otherwise stated, the temperature was kept constant at 23.5±0.5˚C, pH was 6.8, crossflow velocity was 0.12 m/s, and the flux was adjusted to 18 L/m^{2}h (named hereinafter as the baseline operational conditions). During baseline operational conditions the corresponding pressure for the RO membrane was 4.2±0.3 bar and 2.2±0.1 bar for the NF membrane.

Stock solutions of all DBPs were first diluted in approximately 50 mL of background electrolyte solution which was then added into the concentrate line leading to the feed reservoir for final mixing. The baseline DBP concentrations in the 14 L reservoir were 20 µg/L for I-THMs and 50 µg/L for all others. To ensure steady state prior to measurement of rejection as a function of the variable parameters, the membrane was first conditioned by continuously recirculating both permeate and concentrate for 6 days. Experiments investigating the effect of operational factors were then conducted in a randomized order to avoid systematic bias. During the course of permeate sampling lasting 15 minutes, two feed samples were taken headspace-free after 7.5 and 15 minutes and mixed before final extraction.

2.4 Multiple linear regression

Multiple linear regression (MLR), a statistical analysis tool, was applied to the experimental results to determine which physico-chemical properties contributed significantly to DBP rejection. DBP properties represent the predictors of their behaviour and their rejection is the single response variable. Based on purely mathematical criteria, predictors were selected with all possible combinations starting with that which has the highest simple correlation with the response. If the outcome of the prediction was significantly improved, this predictor was retained and the procedure was repeated. A good model will explain as much of the variance of the DBP rejection as possible using the smallest number of predictors. The predictor selection procedure used a sequence of partial F tests to evaluate the significance of a variable. F ratio was calculated by dividing the average improvement in prediction by the model by the average difference between the model and observed data. An increasing F ratio indicates if the initial model significantly improved in predicting DBP rejection. R^2 correlation accounts for how much of the variability in the outcome was accounted for by the predictors. An improved correlation meant more of the variation in DBP rejection was explained by the new added predictors. For the final model, the predictors were selected in terms of explaining a large amount of the variation in DBP rejection at the same time the F ratio ($p<0.01$) still significantly improved DBP rejection prediction. The variance inflation factor (VIF) was used as indicator for multicollinearity. The parameters chosen for this model did not show multicollinearity as the VIFs for all MLRs was below 4 (Table SI-2). Various recommendations for acceptable levels of VIF have been published in the literature, ranging between 4 and 10 [39,40]. All predictors were standardized prior to the regression procedure to remove dependence on units of measurements making them more directly comparable so as to provide a better insight into the importance of the individual predictors in the model.

3. Results and Discussion

3.1. Preliminary experiments

Preliminary experiments investigated the losses of DBPs in the experimental set up due to volatilisation, hydrolysis and adsorption (Figure SI-1) and the time required to reach steady state rejection during membrane filtration (Figure SI-2). Detailed results and descriptions are presented in the SI. Although the experimental set up was solely built of stainless steel, glass and Teflon with a floating lid in the feed tank, losses of DBPs due to volatilisation, hydrolysis and adsorption could not be prevented. Except for TCAN, CH and TCNM which had to be

re-spiked into the system after 3 days, the concentrations of other DBPs were sufficiently high for the investigation of their rejection by the RO and NF membranes. Samples were collected at the same time from the sample collection ports in the feed and the permeate sides of the membrane to calculate rejection at a given time. Time dependency of DBP rejection in the early stages of membrane treatment was observed and taken into account during subsequent experiments (Figure SI-2). For this reason, it was decided that all rejection tests would be carried out after a minimum of 6 days of equilibration time.

3.2 DBP rejection by RO and NF membranes

3.2.1 Reverse osmosis versus nanofiltration

Figure 2 shows DBP rejection by the RO and the NF membrane after reaching steady state at baseline conditions. DBP rejection by RO and NF membranes varied widely from 0 to almost 100% although the rejection for all DBPs was considerably higher for RO than NF. NF membranes are developed with a larger pore size than RO membranes to perform with a higher water permeability which results in reduced rejection characteristics for smaller, less charged ions (e.g. NaCl) compared to RO membranes [41]. Therefore, NF membranes are believed to be 'looser' and their larger pore size is likely to contribute to the higher water permeability. However, pores in the active surface layer of RO and NF membranes should be imagined rather as material-free void spaces in the dense polymer layer, representing tortuous paths for the solute and solvent to pass through [42]. Consequently, the overall lower DBP rejection by NF appears to be related to size exclusion as well as solute-membrane-affinity. Solutes with a high affinity for the membrane material can adsorb onto and partition into the membrane matrix more easily, facilitating diffusion through the membrane matrix [10,43]. The partitioning can take place via hydrophobic interaction or the formation of H-bonds. Hence, solutes which are hydrophobic and/or possess H-bonding moieties might be less rejected by high pressure membranes. HAcAms for example possess two H-bonding donor as well as acceptor sites, which can form H-bonds with the membrane polymer and subsequently facilitate their diffusion to the permeate side. The membrane polymers are made of polyamide which is polarized due to the amine and oxygen in the structure. The extra H-bonding capacity and resulting higher dipole moment may lead to the lower solute rejection through both membranes compared to DBPs with similar molecular size such as CH, HKs, and HNMs.

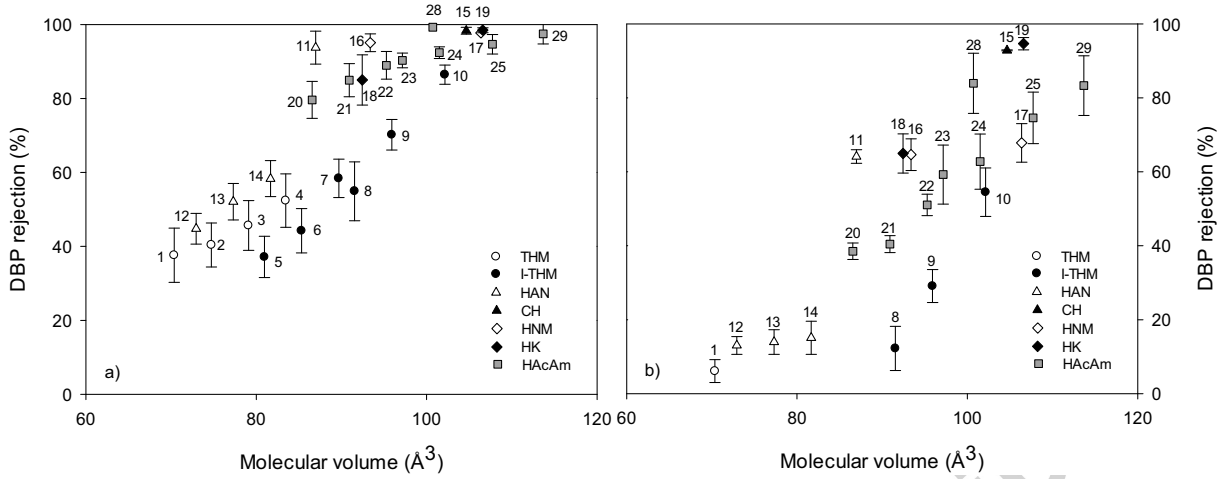

Figure 2 DBP rejection by a) RO and b) NF as a function of molecular volume for baseline conditions at steady state. Error bars indicate the standard deviation between different coupons, RO n=8 and NF n=4. Numbering indicates the individual DBP listed in Table 1.

The smallest DBPs in the suite studied were the THMs and DHANs. Molecular volumes were calculated based on the van der Waals volume of the conformer (ACD/PhysChem Suite). Less than 20% of the DHANs, which have similar molecular volumes to THMs, were rejected by the NF membrane, whereas the THMs, DCIM, BCIM, and DBIM passed completely. THMs and I-THMs are hydrophobic and so, as previously discussed, hydrophobic adsorption may be facilitating the passage of these specific DBPs. The membrane polymer contains both hydrophobic and polar sites for the DBPs to interact with. The large pore size of the NF membrane offers a facilitated entry into the pore and the internal surface area allows DBP adsorption and subsequent easier diffusion to the permeate side. For comparison, the adsorption of hydrophobic hormones has also been found to increase with increasing pore size [44]. As the active surface layer of the RO membrane is also made of polyamide, similar DBP-membrane interaction may occur. Therefore, in addition to size exclusion, adsorption by hydrophobic interaction or H-bonding may also negatively influence DBP rejection by RO.

Table 1 DBP properties, MW = Molecular weight (g/mol), MV = Molecular volume (Å^3), MWidth = Molecular width (Å), DM = Dipole moment (Debye), k_{HYD} = (1/h), K_H = (atm-m^3/mole), H-Acc = H-bond acceptor. [a] Source: ACD/PhysChem Suite, [b] Predicted: ChemBio3D Ultra 12.0, [c] Source: EPIsuite, [d] pH 7.2, 20°C [62], [e] pH 7.0 [63], [f] pH 7.3 [64], [g] 21°C [65], [h] pH 7.0 [66], [i] pH 7.0, 25°C [67].

Disinfection by-product	Abbrev.	MW	MV[a]	MWidth[a]	DM[b]	H-Acc	Log K_{ow}[c]	k_{HYD}	K_H[c]
(1) Chloroform	TCM	119	70	2.38	1.72	0	1.97	[c] $6.45*10^{-5}$	$3.67*10^{-3}$
(2) Bromodichloromethane	BDCM	164	75	2.44	1.82	0	2.10	[c] $1.18*10^{-3}$	$2.12*10^{-3}$
(3) Dibromochloromethane	DBCM	208	79	2.54	1.66	0	2.16	[c] $3.14*10^{-4}$	$7.83*10^{-4}$
(4) Bromoform	TBM	253	83	2.52	1.19	0	2.40	[c] $3.65*10^{-5}$	$5.35*10^{-4}$
(5) Dichloroiodomethane	DCIM	211	81	2.47	2.10	0	2.03	[i] $2.88*10^{-7}$	$6.82*10^{-4}$
(6) Bromochloroiodomethane	BCIM	255	85	2.57	1.80	0	2.11	-	$2.23*10^{-4}$
(7) Dibromoiodomethane	DBIM	300	90	2.57	1.19	0	2.20	-	$7.30*10^{-5}$
(8) Chlorodiiodomethane	CDIM	302	92	2.47	1.84	0	2.53	-	$1.45*10^{-4}$
(9) Bromodiiodomethane	BDIM	347	96	2.56	1.09	0	2.62	-	$4.73*10^{-5}$
(10) Triiodomethane	TIM	394	102	2.59	0.88	0	3.03	-	$3.06*10^{-5}$
(11) Trichloroacetonitrile	TCAN	144	87	2.92	1.33	1	2.09	[d] $6.26*10^{-2}$	$1.34*10^{-6}$
(12) Dichloroacetonitrile	DCAN	110	73	2.43	2.44	1	0.29	[e] $1.87*10^{-3}$	$3.79*10^{-6}$
(13) Bromochloroacetonitrile	BCAN	154	77	2.44	2.69	1	0.38	[f] $1.20*10^{-3}$	$1.26*10^{-6}$
(14) Dibromoacetonitrile	DBAN	199	82	2.52	2.73	1	0.47	[f] $8.15*10^{-4}$	$4.06*10^{-7}$
(15) Chloral hydrate	CH	165	105	3.12	2.33	2	0.99	[c] $1.00*10^{-3}$	$5.71*10^{-9}$
(16) Chloropicrin	TCNM	164	93	3.09	2.21	3	2.09	[c] $4.60*10^{-2}$	$2.05*10^{-3}$
(17) Bromopicrin	TBNM	298	106	3.18	3.13	3	1.59	-	$6.45*10^{-8}$
(18) 1,1-Dichloropropanone	1,1-DCP	127	92	2.84	1.14	1	0.20	[g] $2.20*10^{-2}$	$6.15*10^{-6}$
(19) 1,1,1-Trichloropropanone	1,1,1-TCP	161	107	3.01	2.82	1	1.12	[h] $6.40*10^{-1}$	$2.17*10^{-6}$
(20) Dichloroacetamide	DCAcAm	128	87	2.71	2.17	2	0.19	-	$1.39*10^{-9}$
(21) Bromochloroacetamide	BCAcAm	172	91	2.96	2.36	2	0.00	-	$4.54*10^{-10}$
(22) Dibromoacetamide	DBAcAm	217	95	2.83	2.61	2	0.09	-	$1.49*10^{-10}$
(23) Chloroiodoacetamide	CIAcAm	219	97	2.79	2.35	2	0.41	-	$2.94*10^{-10}$
(24) Bromoiodoacetamide	BIAcAm	264	102	2.91	2.70	2	0.50	-	$9.62*10^{-11}$
(25) Diiodoacetamide	DIAcAm	311	108	2.89	2.86	2	0.92	-	$6.23*10^{-11}$
(26) Bromodichloroacetamide	BDCAcAm	207	105	3.04	2.67	2	-	-	-
(27) Dibromochloroacetamide	DBCAcAm	251	109	3.10	3.12	2	-	-	-
(28) Trichloroacetamide	TCAcAm	162	101	3.06	3.71	2	1.04	-	$4.89*10^{-10}$
(29) Tribromoacetamide	TBAcAm	296	114	3.28	3.48	2	1.10	-	$1.71*10^{-11}$

3.2.2 Multiple linear regression

As indicated by the different DBP behaviours on the membranes, size exclusion and solute-membrane interaction may play an important role in explaining the rejection processes. The mechanisms can be influenced by intrinsic DBP properties. Hence, for understanding which of the various DBP properties most influence the rejection, MLR was performed. Sorption potential was indicated by a solute's solubility in water and its log K_{ow}. Polar surface area, H-bond acceptor sites, H-bond donor sites, polarizability, and dipole moment were chosen to account for polarity and the capacity of the DBP to participate in H-bonding. For the RO membrane, molecular weight (MW), molecular volume (MV), polar surface area (PSA), and dipole moment (DM) were the predictors found to be significant at the 95% confidence interval ($p<0.05$ at $n=29$) with an adjusted R^2 value of 0.938 and F ratio of 99 of the model. No multicollinearities were observed between the predictors. The summary of the regression for each of the 4 predictors is shown in Table SI-2 and these values are used to calculate the predicted rejection in equation (1):

$$Rejection\_RO\ (\%) = 73.3 + 19.9\,MV + 11.0\,PSA - 7.6\,DM - 6.2\,MW \qquad (1)$$

The predictor coefficients in the equation indicate the individual contribution of each predictor to the model. As the size exclusion mechanism directly links to molecular size, a solute with higher molecular volume would lead to its increased rejection. This trend is represented by the positive relationship of MV in equation (1) which affects DBP rejection the most and appears to be a well suited geometric parameter for rejection description. Although MW has previously been correlated with organic solute rejection [11,31], MV may in fact be a better surrogate for molecular size since heavy bromine and/or iodine atoms in many DBPs have more of an impact on density than volume explaining the negative coefficient for MW. This is also clearly evidenced by the macroscopic properties of the molecules TIM, TBM and TCM which have respective densities of 4.01, 2.89 and 1.48 g/cm^3 but whose MVs are 102, 83, and 70 Å^3. CDIM with a MW of 302 g/mol is the third largest of the suite of DBPs in terms of MW but the median of the MV dataset and it shows a rather low rejection of 55%. The rest of the I-THMs show similar behaviour. Properties describing polarity of the DBPs complement the molecular size and geometry in equation (1) since the DBPs have several functional groups. The hydroxyl groups in CH and the nitrile, nitro, or amine group in HANs, HNMs and HAcAms, respectively, provide polar surface areas and

increased dipole moments. I-THMs and THMs showed a decreasing rejection with increasing DM, which lead to a negative correlation of DM in the equation.

When performing MLR for the DBP rejection by the NF membrane, only predictors related to molecular size (i.e. MW and MV) appeared to be significant for a good description of rejection ($R^2 = 0.928$), as shown in equation (2)

$$Rejection\_NF\ (\%) = 40.0 + 37.0MV - 18.0MW \qquad (2)$$

The pore size of the NF90 has been estimated in different studies to be in the range of 0.34 - 0.38 nm [10,45,46]. Since all the DBPs are smaller than or in the range of the membrane pore size (Table 1), size exclusion is likely to be a dominant mechanism and this is indicated in equation (2).

3.3 Impact of operational parameters on the rejection of DBPs

Although the rejection of THMs, I-THMs, DHANs, CH, HKs and HAcAms was measured as a function of operational parameters for both membranes, the behaviour of BCAN, DCAcAm, 1,1,1-TCP and TIM is selected for description in subsequent figures as these DBPs represent the different functionalities and properties of all chemicals tested. BCAN represents the small polar HANs that showed low rejection. DCAcAm is a midsize molecule with median rejection and represents the polar HAcAms which possess H-bonding/accepting capacity. 1,1,1-TCP was chosen as one of the largest molecules with highest rejection among the DBPs evaluated. TIM is the most hydrophobic DBP in the suite. The behaviour of all DBPs measured as a function of the different operational parameters is shown in the Supporting information (Figure SI-3 to SI-12).

3.3.1 Transmembrane flux

Figure 3 shows the effect of transmembrane flux for both membranes on the rejection of BCAN, DCAcAm, 1,1,1-TCP and TIM. The pressure increase with increased flux should not have caused any significant changes in the membrane effective pore size as the membrane was previously at higher pressures than those used here.

Overall, with the RO membrane the rejection of all DBPs, except TIM, increased with increasing transmembrane flux. However, the degree, to which transmembrane flux impacted rejection, varied depending on the group of DBPs with the greatest impact occurring for the THMs and the HANs. For HANs, HAcAms, 1,1-DCP, CH and HNMs the greatest impact in rejection was seen at fluxes between 3 and 18 L/m^2h. At higher values, rejection remained

relatively stable. Because the diffusive flux of the larger DBPs (e.g. 1,1,1-TCP, CH, TCNM, BIAcAm, DIAcAm, BDCAcAm, DBCAcAm, TCAcAm, TBAcAm) is always low, they were marginally affected (<8%) by the changes in transmembrane flux. The diffusive flux through a membrane occurs due to a concentration difference, whereas the convective flux of solutes is caused by pressure differences [47]. Besides the THMs, the HANs are the smallest DBPs in the suite studied. Therefore, at higher transmembrane fluxes the diffusive flux of those DBPs is small compared to the water flux which in turn leads to low concentrations in the permeate as a result of higher rejection. THM rejection on the other hand, continuously increased over the full range of transmembrane fluxes studied up to 60-70%. The increased solute-membrane affinities within the iodo-THMs due to their increasing hydrophobicity with increasing number of iodine atoms, led to a decreased variation of rejection with increasing permeate flux (Figure SI-5). In particular TIM did not show a change in rejection. To maintain similar rejection values over the flux range, the diffusive flux needs to increase with increasing permeate flux. As proposed by Déon *et al.* [48], increasing pressure (inducing the higher flux) can increase the solute concentration on the membrane surface, which in turn leads to a higher concentration gradient and a decrease in rejection.

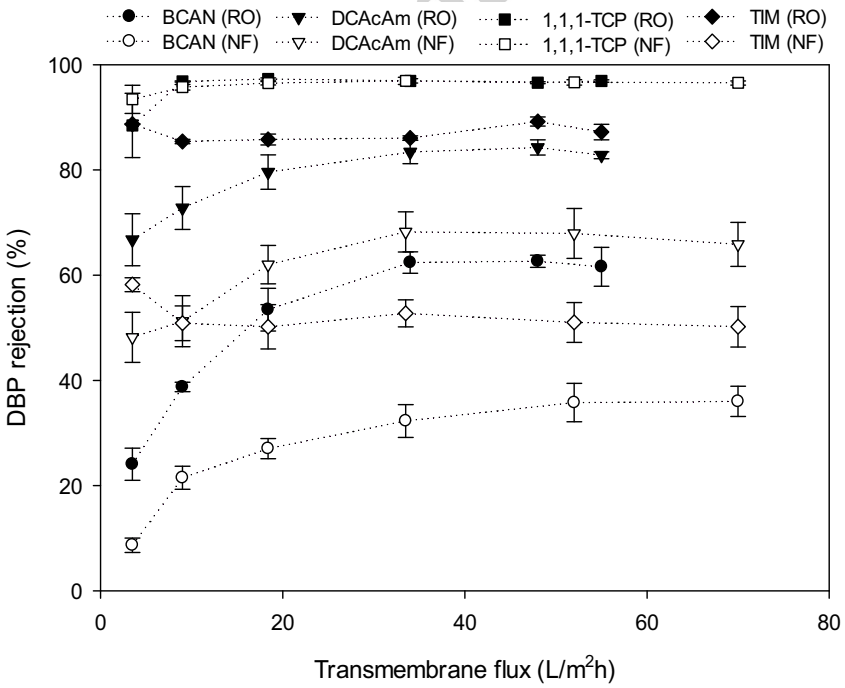

Figure 3 Rejection of BCAN, DCAcAm, 1,1,1-TCP and TIM as a function of transmembrane flux. Error bars indicate the propagation of uncertainty between duplicate samples (feed pH 6.8, crossflow velocity 0.12 m/s, 7 mM NaCl, 1 mM KH_2PO_4, feed temperature 23.5˚C).

Similarly to the RO membrane, the rejection of all DBPs by the NF membrane was most sensitive to changes at fluxes below 18 L/m^{2}h. The THM4 and the three I-THMs DCIM, BCIM, and DBIM were not rejected at baseline conditions but decreased concentrations in the permeate could be seen starting at 35 L/m^{2}h with a maximum rejection of 25% at a permeate flux of 70 L/m^{2}h. BDIM and TIM were not affected by changes in the permeate flux contrary to the other DBPs including CDIM which showed increasing rejection with increasing transmembrane flux. For TIM the highest rejection of 58% in the flux range was actually observed at the lowest flux, due to the chemical's adsorptive interactions with the membrane. DCAcAm with a log K_{ow} 0.2 has minimal hydrophobic adsorptive interactions and, hence, a relatively wide range of rejection as a function of transmembrane flux is expected. This occurs due to the diffusive solute flux being rather large compared to the solvent flux at low transmembrane fluxes, while at higher transmembrane fluxes the solute flux becomes small compared to the water flux. The rejection increase levelled off at 35 L/m^{2}h as increasing transmembrane flux and therefore increasing pressure possibly led to a higher concentration gradient and subsequent higher permeation. As with the RO membrane, the larger well rejected DBPs 1,1,1-TCP, CH, BDCAcAm, DBCAcAm, TCAcAm, TBAcAm show only little variation in rejection on the NF membrane over the flux range studied.

3.3.2 Crossflow velocity

Figure 4 shows DBP rejection by the RO and NF membrane as a function of crossflow velocity. An increase in crossflow velocity of the feed solution leads to a greater mixing at the membrane surface and decreased concentration polarisation [49] should, therefore, result in increased DBP rejection. Changes from 0.04 to 0.16 m/s across the RO membrane resulted in an 8-11% increase in rejection for DHANs and 5% for DCAcAm, which is greater than the experimental error for these smaller molecules. As stated above, this can be explained by increased cross flow velocity reducing concentration polarization at the membrane-bulk solution interface [50]. The increase in crossflow velocity can decrease the thickness of the concentration polarisation layer contrary to what is induced by a pressure increase. This change in concentration polarisation layer thickness contributes to the rejection increase observed experimentally. On the other hand, larger DBPs (HKs, HNMs, CH, and the remaining HAcAms) and those which tend to interact with the membrane polymer (THMs and I-THMs) were not affected by changes in cross flow velocity. The adsorption of THMs and I-THMs into the RO membrane material will cause their concentration to be higher on the membrane surface than in the polarization layer. Subsequently, they will not be affected

by changes in the concentration polarisation layer induced by increased turbulence with increasing crossflow velocity. Changes in crossflow velocity did not influence the rejection of DBPs by the NF membrane.

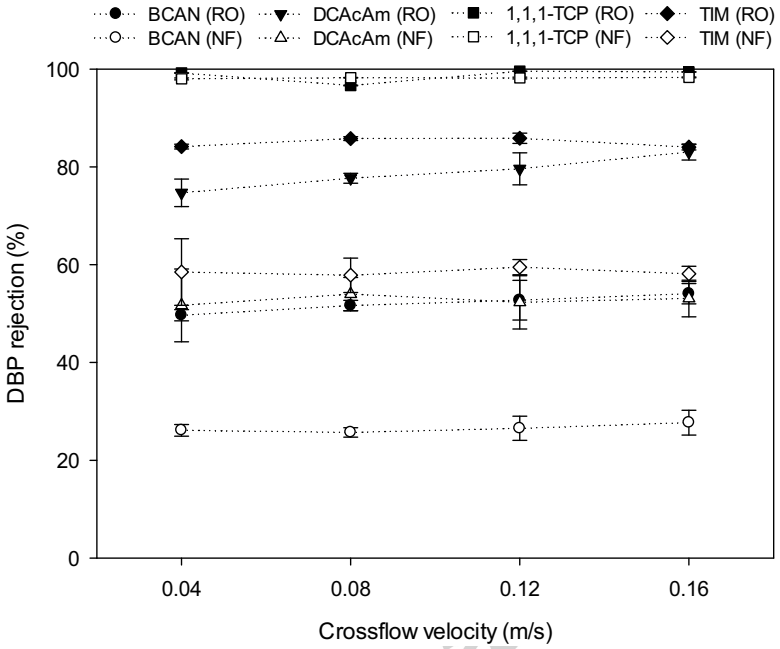

Figure 4 Rejection of BCAN, DCAcAm, 1,1,1-TCP and TIM as a function of crossflow velocity. Error bars indicate the propagation of uncertainty between duplicate samples (permeate flux 18 L/m^{2}h, feed pH 6.8, 7 mM NaCl, 1 mM KH_2PO_4, feed temperature 23.5˚C).

3.3.3 Temperature

Figure 5a shows DBP rejection as a function of temperature where a temperature increase between 23˚C and 35˚C led to a decrease of the rejection of BCAN by the RO membrane from 47 to 26% and for TIM from 88% to 70%. Besides membrane permeability increased with increasing temperature and salt rejection decreased 0.5% for RO and 2.5% for NF across the temperature range (Figure SI-13).

These observations are in accordance with previous studies which also observed an increased neutral solute passage and permeability with increased temperature at constant flux [51,52]. The decreased rejections may be a result of the thermal expansion of the active membrane surface layer. Previous research reported polymer relaxation at elevated temperatures which subsequently reduced the filtration hindrance of neutral solutes [53,54]. The contribution of increasing pore size is supported by the increase of permeability when correcting for viscosity (Figure SI-13).

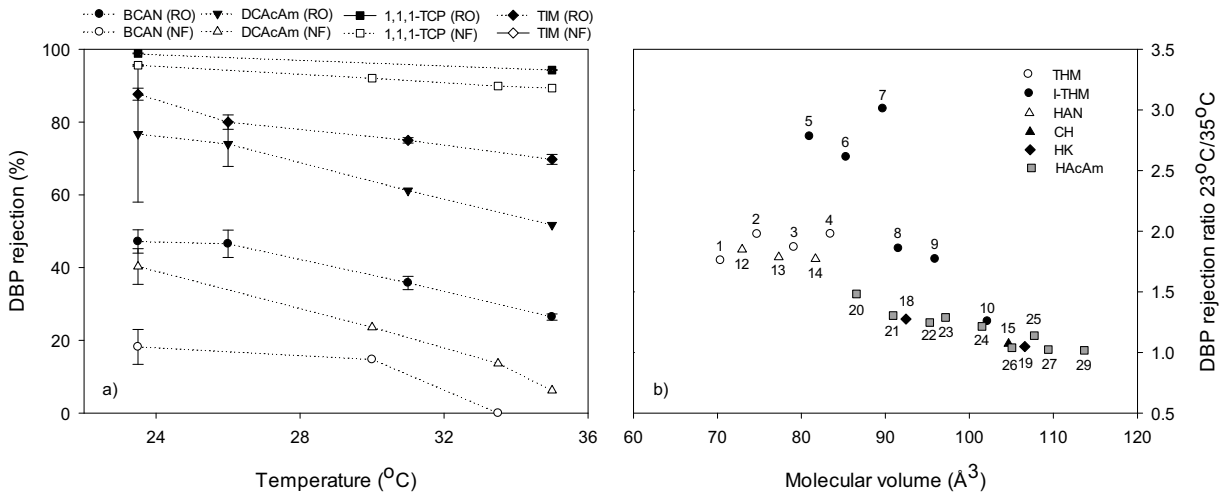

Figure 5 a) Membrane rejection of BCAN, DCAcAm, 1,1,1-TCP and TIM as a function of temperature, where error bars indicate the propagation of uncertainty between duplicate samples, b) DBP rejection by RO membrane as ratio (23˚C to 35˚C) related to molecular volume (permeate flux 18 L/m^{2}h, feed pH 6.8, crossflow velocity 0.12 m/s, 7 mM NaCl, 1 mM KH_2PO_4). Numbering indicates the individual DBP which are listed in Table 1.

In Figure 5b the impact of a temperature increase from 23˚C to 35˚C is scaled and related to the molecular volume. The results suggest that the impact becomes greater with smaller molecular volume because an expanding effective pore size can better facilitate the entry of small molecules into the membrane matrix. In addition to the increased pore size, an increase in diffusion rate into the membrane matrix caused by the decrease in viscosity of the water-DBP solution may contribute to the lower DBP rejection. Moreover, high temperatures were found to increase partitioning [55] which could be the reason why the I-THMs are impacted more by a change in temperature compared to other DBPs of similar size (Figure 5b).

3.3.4 pH

The active polyamide membrane surface layer contains amine, hydroxyl and carboxylic functional groups which may affect the solute rejection mechanism upon changes in the solution pH. It has been reported that in the range of acidic to basic pH values, changes in the membrane structure can occur. This structural change is attributed to stronger electrostatic interactions between the dissociated functional groups leading to a pore shrinkage at high pH [46]. Contrary to pore shrinkage, an increase in pore size with increasing pH was proposed in literature [56]. In this current study, the permeability of the NF membrane decreased gradually from pH 4.5 through 5.5 and from 7 to 8.5 by 0.3 L/m^{2}hbar whereas it did not change at all with the RO membrane (Figure SI-14). Due to the greater pore size of the NF as compared to the RO membrane, the salt rejection by NF membranes can be dependent on

both size exclusion and Donnan exclusion [57]. Hence, the impact of pH on salt rejection may be more pronounced for the NF membrane, since Donnan exclusion becomes more important as the membrane surface charge becomes increasingly negative with increasing pH. Since size exclusion is the dominant mechanism of rejection for the RO membrane, the effect of pH on rejection is small.

BCAN with a molecular volume of 77 $Å^3$ is among the smallest DBPs tested and its rejection could, therefore, be affected by minor changes in the void spaces in the RO membrane matrix. However, the observed changes were not significant enough to draw a firm conclusion (see Figure 6). On the other hand, increased rejection of HAcAms with increasing pH was seen with the NF membrane; 16% for DCAcAm, 12% for BCAcAm, 10% for DBAcAm and 10% for CIAcAm. DBP transport through the membrane may be facilitated by H-bonding between the membrane polymer and the DBP. HAcAms, due to their intrinsic functional groups, possess two H-bond donor and acceptor sites. With increasing pH, however, the increased concentration of hydroxide ions can interfere with H-bonding between the membrane and the polar HAcAms leading to an increased rejection.

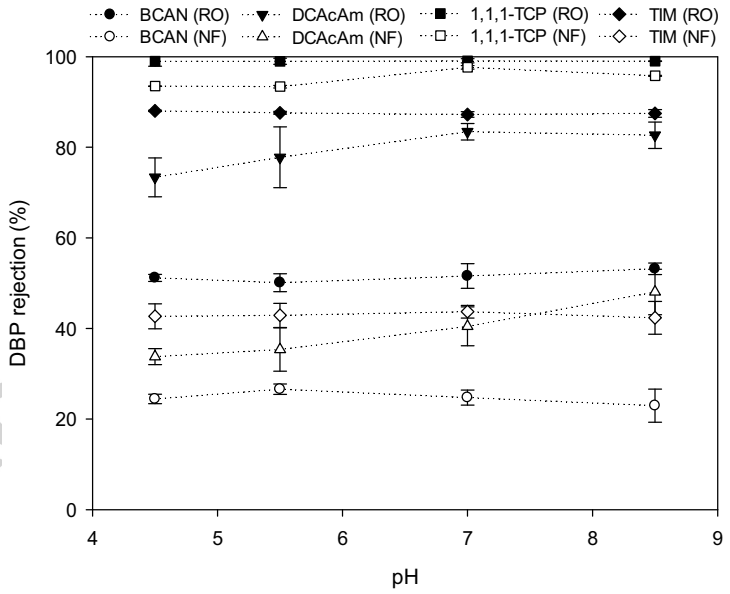

Figure 6 Rejection of BCAN, DCAcAm, 1,1,1-TCP and TIM as a function of pH, where error bars indicate the propagation of uncertainty between duplicate samples (permeate flux 18 L/m^2h, crossflow velocity 0.12 m/s, 7 mM NaCl, 1 mM KH_2PO_4, feed temperature 23.5˚C).

The THMs and I-THMs were not affected by changes in pH during either RO or NF filtration; THMs and I-THMs with log $K_{ow} > 2$ are more hydrophobic than the other DBPs and, therefore, interact more with the membrane. Their removal may be essentially governed

by adsorption, which is not affected by minor changes in either surface charge or pore size of the membranes. Moreover, the feed concentration of the THMs and I-THMs did not vary greater than the analytical error. Therefore, further adsorption or desorption of the THMs and I-THMs due to a change of the equilibrium reached during 6 days of recirculation is not expected to influence rejection.

3.3.5 Ionic strength

Solution ionic strength can affect the properties of both membrane and DBPs. An increased ion concentration may partially increase the screening of the membrane charge (i.e. to some degree, counter-ions in solution may screen the polar functional groups) associated with polar DBPs reducing their hydrodynamic radius and leading to a smaller apparent solute size [58]. Additionally, it was previously reported that an increase in ionic strength may lead to an increase in mean pore size [59]. However, the rejection of all DBPs during RO and NF filtration was not affected when the ionic strength in the feed was increased from 7 mM to 70 mM NaCl. The only exception was the group of HAcAms during NF filtration which showed an increased rejection with increasing ionic strength (Figure 7).

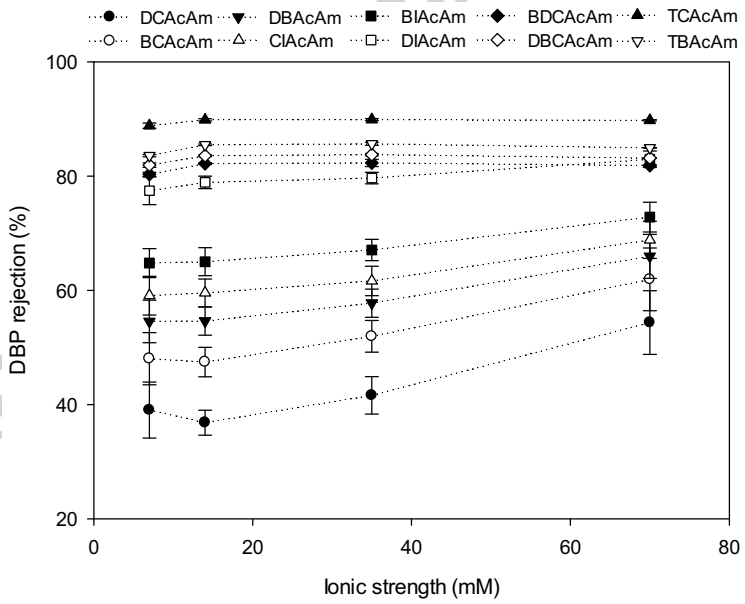

Figure 7 Rejection of HAcAms by NF as a function of ionic strength. Error bars indicate the propagation of uncertainty between duplicate samples (permeate flux 18 L/m^{2}h, feed pH 6.8, crossflow velocity 0.12 m/s, 1 mM KH_2PO_4, feed temperature 23.5˚C).

For example the rejection of DCAcAm increased by 15% with an increase in ionic strength from 7 to 70 mM NaCl. With increasing ionic strength the negative charges on the membrane can be increasingly shielded by counter ions in solution. It has been reported that with

increasing ionic strength of the solution due to the compression of the electrical double layer the overall charge of RO and NF membranes decreases [60,61]. The theory of a lower surface charge caused by the higher ionic strength in solution is in accordance with the observed decreased salt rejection of 1.3% and 5.8% for RO and NF, respectively (Figure SI-14). The impact of ionic strength may have been too small relative to other parameters to induce significant changes in DBP rejection by RO.

The HAcAms have the capacity to interact with the membrane polymer by H-bonding. Therefore, the increasing shielding of the membrane surface charge may lead to less HAcAm-membrane interaction. Due to their polarity, HAcAms possess dipole moments ranging from 2.2 to 3.7 Debye. Van der Bruggen *et al.* [11] suggested that the negative charges of the functional groups on the membrane surface can direct the opposite charge of the dipole of a compound towards the surface and therefore facilitate entry into the pore. The increased rejection with increasing ionic strength may be a result of decreased directing of the HAcAms towards the pore. The highest impact on rejection was seen for DCAcAm with 15%. The effect is reduced for the larger HAcAms, i.e. DIAcAm rejection only increased by 5%. DCAcAm is the smallest and most cylindrical of the HAcAms. Increasing halogen content in the molecule and also the substitution of the smaller chlorine atom with the larger bromine or iodine atom causes the shape of the HAcAms to become longer and more cylindrical (e.g. DCAcAm) and eventually to become a more bulky molecule (e.g TBAcAm).

3.4 Modelling DBP rejection

The effort in identifying influential molecular properties (section 3.2) using MLR was expanded to also include operational parameters with the aim of developing a predictive model for small organic solute rejection by RO, while no attempt was carried out for the NF membrane. Operational parameters, such as transmembrane flux, crossflow velocity, temperature, pH, and ionic strength were included resulting in a large comprehensive dataset with a sample size of 500 measurements. There are several advantages with the large dataset; firstly, a calibration and a subsequent validation of the developed MLR model can be performed with confidence and, secondly, an extremely wide range of rejection values, (i.e. 5-100%) is embraced. One half of the data was used to build the model, and the model was then applied to the other half of the data. Rejection data of two THMs, three I-THMs, two HANs, CH, four HAcAms, and 1,1,1-TCP was used for model calibration (n=286) while the remaining DBP data was used for model validation (n=214). Figure 8 illustrates the

calibration and validation models obtained to describe the DBP rejection depending on molecular properties and operational parameters where the measured rejection is plotted against the predicted rejection. The resulting correlation of calculated and measured data was near identical for the calibration (R_{cal}^2 = 0.922) and the validation (R_{val}^2 = 0.913) dataset, which gives high confidence in the ability of the MLR to predict rejection of small organic contaminants for a broad diversity of operational parameters.

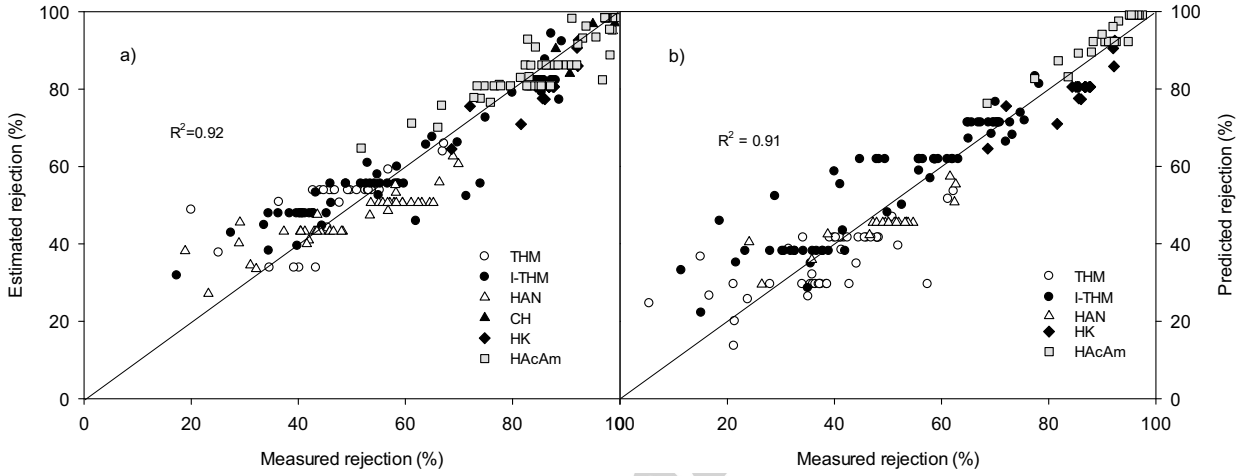

Figure 8 Multiple linear regression a) calibration model and b) validation model of DBP rejection by RO.

Similar to the MLR only using molecular properties (section 3.2) polar surface area (PSA), molecular volume (MV) and dipole moment (DM) were significant at the 95% confidence level. The operational parameters temperature and flux were also significant at the 95% confidence level and complement the linear relationship describing solute rejection (equation 3) with an adjusted quality of fit of R^2=0.901.

$$Rejection(\%) = -38.7 + 0.6\,PSA + 1.5\,MV - 5.9\,DM - 1.3\,Temp + 0.3\,Flux \qquad (3)$$

To allow for intercomparison of the regression coefficients the data was normalized obtaining a similar adjusted quality of fit of R^2=0.922. As provided by the normalized model (equation 4) the impact of the different parameters follows the order PSA > MV > DM > Temperature > Flux. Temperature was found to have a greater impact than transmembrane flux highlighting the importance of temperature changes on the rejection of small organic solutes, especially in regards to its negative correlation.

$$Rejection(\%) = 69.5 + 16.5\,PSA + 15.2\,MV - 10.1\,DM - 3.8\,Temp + 3.6\,Flux \qquad (4)$$

To gain further confidence in the predictive power of the model for other known contaminants which were not used for model development, the obtained relationship (equation 3) was applied to N-Nitrosamine rejection data adapted from Fujioka and co-authors [18]. N-nitrosodimethylamine (NDMA), N-nitrosomethylethylamine (NMEA), and N-Nitrosopyrrolidine (NPyr) which exhibit the lowest rejection out of the group of N-Nitrosamines studied were used for this exercise. Their low rejection and small size make them the most challenging N-Nitrosamines for the model. As seen in Figure 9 the developed model successfully simulated N-Nitrosamine rejection across a wide range of rejection, temperatures (10-40˚C) and transmembrane fluxes (5-60 L/m^{2}h).

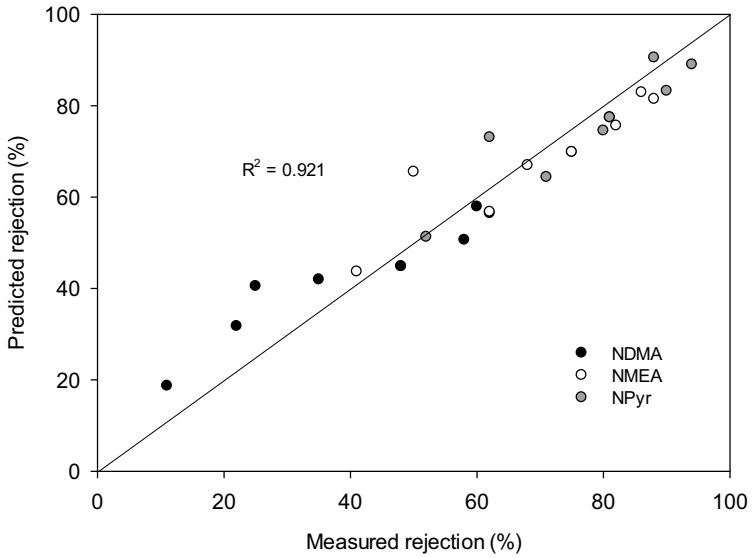

Figure 9 Comparison of the application of rejection data obtained with the developed MLR and measured N-Nitrosamine rejection data adapted from Fujioka and co-authors [18] using RO membranes.

4. Conclusions

Multiple linear regression (MLR) could successfully describe DBP rejection by RO and NF. While geometric parameters were revealed to be good descriptors during NF filtration, properties related to polarity significantly influenced rejection by RO, indicating that steric hindrance is the major removal mechanism for NF but solute-membrane interaction strongly contributes to rejection by RO. Increasing transmembrane flux led to increased rejection of all DBPs (except TIM) by RO and BDIM and TIM by NF due to their hydrophobic interactions with the membrane, while the greatest change in rejection was observed, when modifying transmembrane flux below 18 L/m^{2}h. Increasing temperature (23.5 to 35˚C) led to

a considerable drop in rejection for all DBPs. Smaller molecular size would lead to an increasingly negative impact of temperature which was most pronounced for the I-THMs due to a combination of polymer expansion and enhanced partitioning. No discernible impact on rejection by both membranes with change in crossflow velocity was observed for all the DBPs. Only DHAN and DCAcAm rejection increased with increasing crossflow velocity during RO filtration which is related to reduced concentration polarisation. pH in the range 4.5 to 8.5 did not influence the rejection of the DBPs by RO while the rejection of HAcAms by NF membranes increased likely due to hydroxide ions interfering with H-bonding between the membrane and the DBP. No discernible impact on DBP removal was seen with increases in ionic strength (7 to 70 mM) by either RO or NF membranes, but led to an increased HAcAms rejection of up to 15% for DCAcAm by NF likely due to reduced polar interaction with the membrane polymer. A multiple linear regression model for rejection prediction at various operational conditions was developed and validated. The developed model can successfully predict the rejection by simply using a linear relationship of three common molecular properties, the transmembrane flux and temperature. The modelled results revealed temperature to be the major influencing operational parameter. Modelled DBP rejection data was in good agreement with experimentally determined rejection data obtained during this study as well as N-Nitrosamine data adapted from a different study. Together this gives great confidence in the ability of the simple model to predict rejection of small organic contaminants for a broad diversity of operational parameters including the rejection of other known compounds that were not used to develop the model.

Acknowledgements

The authors gratefully acknowledge the support of the WateReuse Research Foundation (U.S.A.), Veolia Water (Australia) and Seqwater's financial, technical, and administrative assistance in funding and managing the project WaterReuse-10-18, within which this manuscript was developed. In particular we appreciate the valuable comments and support from the Project Advisory Committee - Stuart Khan, Christopher Bellona, Daniel Gerrity and Stuart Krasner.

References

[1] N.N. Li, Advanced membrane technology and applications, John Wiley & Sons, New Jersey, 2008.

[2] J. Drewes , S. Kahn, Chapter 16: Water Reuse for Drinking Water Augmentation, in, Water Resources and Environmental Engineering: Water Quality and Treatment: A Handbook on Drinking Water (6th Edition), McGraw-Hill Professional Publishing New York, NY, USA 2011.

[3] H.K. Shon, S. Vigneswaran, S.A. Snyder, Effluent Organic Matter (EfOM) in Wastewater: Constituents, Effects, and Treatment, Environ. Sci. Technol. 36 (2006) 327-374.

[4] A. Matin, Z. Khan, S.M.J. Zaidi, M.C. Boyce, Biofouling in reverse osmosis membranes for seawater desalination: Phenomena and prevention, Desalination 281 (2011) 1-16.

[5] H.-C. Flemming, Reverse osmosis membrane biofouling, Exp. Therm. Fluid Sci. 14 (1997) 382-391.

[6] S.D. Richardson, M.J. Plewa, E.D. Wagner, R. Schoeny, D.M. DeMarini, Occurrence, genotoxicity, and carcinogenicity of regulated and emerging disinfection by-products in drinking water: A review and roadmap for research, Mut. Res. 636 (2007) 178-242.

[7] D.L. Sedlak, U. Von Gunten, The chlorine dilemma, Science 331 (2011) 42-43.

[8] S.W. Krasner, P. Westerhoff, B. Chen, B.E. Rittmann, G. Amy, Occurrence of Disinfection Byproducts in United States Wastewater Treatment Plant Effluents, Environ. Sci. Technol. 43 (2009) 8320-8325.

[9] K. Doederer, W. Gernjak, H.S. Weinberg, M.J. Farré, Factors affecting the formation of disinfection by-products during chlorination and chloramination of secondary effluent for the production of high quality recycled water, Water Res. 48 (2014) 218-228.

[10] V. Yangali-Quintanilla, A. Sadmania, M. McConvillea, M. Kennedya, G. Amy, Rejection of pharmaceutically active compounds and endocrine disrupting compounds by clean and fouled nanofiltration membranes." Water Res. 43 (2009) 2349-2362.

[11] B. Van der Bruggen, J. Schaep, D. Wilms, C. Vandecasteele, Influence of molecular size, polarity and charge on the retention of organic molecules by nanofiltration, J. Membr. Sci. 156 (1999) 29-41.

[12] P. Berg, G. Hagmeyer, R. Gimbel, Removal of pesticides and other micro-pollutants by nanofiltration, Desalination 113 (1997) 205-208.

[13] L.D. Nghiem, A.I. Schäfer, M. Elimelech, Pharmaceutical retention mechanisms by nanofiltration membranes, Environ. Sci. Technol., 39 (2005) 7698-7705.

[14] K. Kimura, G. Amy, J.E. Drewes, T. Heberer, T.-U. Kim, Y. Watanabe, Rejection of organic micropollutants (disinfection by-products, endocrine disrupting compounds, and pharmaceutically active compounds) by NF/RO membranes, J. Membr. Sci., 227 (2003) 113-121.

[15] Y. Kiso, Y. Nishimura, T. Kitao, K. Nishimura, Rejection properties of non-phenylic pesticides with nanofiltration membranes, J. Membr. Sci., 171 (2000) 229-237.

[16] J.Y. Hu, X. Jin, S.L. Ong, Rejection of estrone by nanofiltration: influence of solution chemistry, J. Membr. Sci., 302 (2007) 188-196.

[17] V. Uyak, I. Koyuncu, I. Oktem, M. Cakmakci, I. Toroz, Removal of trihalomethanes from drinking water by nanofiltration membranes, J. Haz. Mat. 152 (2008) 789-794.T.

[18] T. Fujioka, L.D. Nghiem, S.J. Khan, J.A. McDonald, Y. Poussade, J.E. Drewes, Effects of feed solution characteristics on the rejection of N-nitrosamines by reverse osmosis membranes, J. Membr. Sci. 409-410 (2012) 66-74.

[19] J.E. Drewes, C. Bellona, Y. Xu, G. Amy, T.-U. Kim, Rejection of Wastewater-Derived Micropollutants in High-Pressure Membrane Applications Leading to Indirect Potable Reuse, in, Water Reuse Foundation, Alexandria, Virginia, 2006.

[20] P. Xu, J.E. Drewes, C. Bellona, G. Amy, T.-U. Kim, M. Adam, T. Heberer, Rejection of Emerging Organic Micropollutants in Nanofiltration–Reverse Osmosis Membrane Applications, Water Environ. Res., 77 (2005) 40-48.

[21] E. Steinle-Darling, Rejection of trace organics - nitrosamines, perfluorochemical, and others - via reverse osmosis and nanofiltration, in, Civil and Environ, Engineering, Stanford University, 2008.

[22] Fujioka, S.J. Khan, J.A. McDonald, A. Roux, Y. Poussade, J.E. Drewes, L.D. Nghiem, N-nitrosamine rejection by reverse osmosis membranes: A full-scale study, Water Res. (2013).

[23] K.L. Linge, J.W. Blythe, F. Busetti, P. Blair, C. Rodriguez, A. Heitz, Formation of halogenated disinfection by-products during microfiltration and reverse osmosis treatment: Implications for water recycling, Sep. Purif. Technol. 104 (2013) 221-228.

[24] R. Chalatip, R. Chawalit, R. Nopawan, Removal of haloacetic acids by nanofiltration, J. Environ. Sci. 21 (2009) 96-100.

[25] A. Waniek, M. Bodzek, K. Konieczny, Trihalomethane Removal from Water Using Membrane Processes, P. J. Environ. Stud. 11 (2002) 171-178.

[26] E. Agus, D.L. Sedlak, Formation and fate of chlorination by-products in reverse osmosis desalination systems, Water Res. 44 (2010) 1616-1626.

[27] M.J. Farré, K. Döderer, L. Hearn, Y. Poussade, J. Keller, W. Gernjak, Understanding the operational parameters affecting NDMA formation at Advanced Water Treatment Plants, J. Haz. Mat. 185 (2011) 1575-1581.

[28] E. Steinle-Darling, M. Zedd, M.H. Plumlee, H.F. Ridgway, M. Reinhard, Evaluating the impacts of membrane type, coating, fouling, chemical properties and water chemistry on reverse osmosis rejection of seven nitrosoalklyamines, including NDMA, Water Res. 41 (2007) 3959-3967.

[29] J. Almedeij, R. Aljarallah, Seasonal Variation Pattern of Monthly Wastewater Influent, J. Environ. Eng. 137 (2011) 332-339.

[30] A. Escoda, P. Fievet, S. Lakard, A. Szymczyk, S. Déon, Influence of salts on the rejection of polyethyleneglycol by an NF organic membrane: Pore swelling and salting-out effects, J. Membr. Sci. 347 (2010) 174-182.

[31] R.Y. Ning, T.L. Troyer, Colloidal fouling of RO membranes following MF/UF in the reclamation of municipal wastewater, Desalination 208 (2007) 232-237.

[32] K. Doederer, M.J. Farré, J. Keller, W. Gernjak, H.S. Weinberg, Y. Poussade, How to minimize disinfection by-products during the production of High Quality Recycled Water, Water Quality and Technology Conference Proceedings, Phoenix, AZ (2011) 2499-2507.

[33] V. Uyak, I. Koyuncu, I. Oktem, M. Cakmakci, I. Toroz, Removal of trihalomethanes from drinking water by nanofiltration membranes, J. Haz. Mat. 152 (2008) 789-794.

[34] Seqwater, Annual Report 2012-13 for the Western Corridor Recycled Water Scheme - Recycled Water Management Plan (2013). Obtained from the internet: http://www.seqwater.com.au/sites/default/files/PDF%20Documents/Publications/2012-13%20WCRWS%20Annual%20Report.pdf

[35] H.S. Weinberg, S.W. Krasner, S.D. Richardson, A.D.J. Thruston, The Occurrence of Disinfection ByProducts (DBPs) of Health Concern in Drinking Water: Results of a Nationwide DBP Occurence Study, in, U.S. Environmental Protection Agency, Athens, GA, 2002.

[36] T. Fujioka, S.J. Khan, Y. Poussade, J.E. Drewes, L.D. Nghiem, N-nitrosamine removal by reverse osmosis for indirect potable water reuse – A critical review based on observations from laboratory-, pilot- and full-scale studies, Sep. Purif. Technol. 98 (2012) 503-515.

[37] B. Van der Bruggen, M. Mänttäri, M. Nyström, Drawbacks of applying nanofiltration and how to avoid them: A review, Sep. Purif. Technol. 63 (2008) 251-263.

[38] C. Ayache, M. Pidou, W. Gernjak, Y. Poussade, J.-P. Croué, A. Tazi-Pain, J. Keller, Characterization of secondary treated effluents for tertiary membrane filtration and water recycling, J. Water Reuse Desalination 2 (2012) 74–83.

[39] J.F.J. Hair, R.E. Anderson, R.L. Tatham, W.C. Black, Multivariate Data Analysis 3rd ed., Macmillan, New York, 1995.

[40] Y. Pan, R.T. Jackson, Ethnic difference in the relationship between acute inflammation and and serum ferritin in US adult males, Epidemiol. Infect. 136 (2008) 421-431.

[41] R. Bergman, Reverse osmosis and nanofiltration, American Water Works Association, Denver, CO, 2007.

[42] P. Meares, The physical chemistry if transport and separation by membranes, Elsevier, Amsterdam, 1976.

[43] K. Kimura, G. Amy, J.E. Drewes, Y. Watanabe, Adsorption of hydrophobic compounds onto NF/RO membranes: an artifact leading to overestimation of rejection, J. Membr. Sci. 221 (2003) 89-101.

[44] A.J.C. Semião, A.I. Schäfer, Removal of adsorbing estrogenic micropollutants by nanofiltration membranes. Part A-Experimental evidence, J. Membr. Sci. 431 (2013) 244-256.

[45] C. Bellona, J.E. Drewes, The role of membrane surface charge and solute physico-chemical properties in the rejecion of organic acids by NF membranes, J. Membr. Sci. 249 (2005) 227-234.

[46] M.J. López-Muñoz, A. Sotto, J.M. Arsuaga, B. Van der Bruggen, Influence of membrane, solute and solution properties on the retention of phenolic compounds in aqueous solution by nanofiltration membranes, Sep. Purif. Technol. (2009) 194-201.

[47] K.S. Spiegler, O. Kedem, Thermodynamics of hyperfiltration (reverse osmosis): criteria for efficient membranes, Desalination 1 (1966) 311-326.

[48] S. Déon, P. Dutournié, P. Fievet, L. Limousy, P. Bourseau, Concentration polarization phenomenon during the nanofiltration of multi-ionic solutions: Influence of the filtrated solution and operating conditions, Water Res. 47 (2013) 2260-2272.

[49] Z. Amjad, Reverse osmosis: membrane technology, water chemistry & industrial applications, Van Nostrand Reinhold, New York, 1993.

[50] S.P. Nunes, K.V. Peinemann, Membrane Technology in the Chemical Industry, Wiley-VCH, Weinheim, Germany, 2010.

[51] J.M. Arsuaga, M.J. López-Muñoz, J. Aguado, A. Sotto, Temperature, pH and concentration effects on retention and transport of organic pollutants across thin-film composite nanofiltration membranes, Desalination 221 (2008) 253-258.

[52] N. Ben Amar, H. Saidani, A. Deratani, J. Palmeri, Effect of Temperature on the Transport of Water and Neutral Solutes across Nanofiltration Membranes, Langmuir 23 (2007) 2937-2952.

[53] R.R. Sharma, R. Agrawal, S. Chellam, Temperature effects on sieving characteristics of thin-film composite nanofiltration membranes: pore size distributions and transport parameters, J. Membr. Sci. 223 (2003) 69-87.

[54] M. Nilsson, G. Trägårdh, K. Östergren, The influence of different kinds of pre-treatment on the performance of a polyamide nanofiltration membrane, Desalination 195 (2006) 160-168.

[55] A. Tan, A. Ziegler, B. Steinbauer, J. Seelig, Thermodynamics of Sodium Dodecyl Sulfate Partitioning into Lipid Membranes, Biophys. J. 83 (2002) 1547-1556.

[56] B.C. Donose, S. Sukumar, M. Pidou, Y. Poussade, J. Keller, W. Gernjak, Effect of pH on the ageing of reverse osmosis membranes upon exposure to hypochlorite, Desalination 309 (2013) 97-105.

[57] J.M.M. Peeters, J.P. Boom, M.H.V. Mulder, H. Strathmann, Retention measurements of nanofiltration membranes with electrolyte solutions, J. Membr. Sci. 145 (1998) 199-209.

[58] A.I. Schäfer, L.D. Nghiem, T.D. Waite, Removal of the Natural Hormone Estrone from Aqueous Solutions Using Nanofiltration and Reverse Osmosis, Environ. Sci. Technol. 37 (2003) 182-188.

[59] G. Bargeman, J.M. Vollenbroek, J. Straatsma, C.G.P.H. Schroën, R.M. Boom, Nanofiltration of multi-component feeds. Interactions between neutral and charged components and their effect on retention, J. Membr. Sci. 247 (2005) 11-20.

[60] A.E. Childress, M. Elimelech, Effect of solution chemistry on the surface charge of polymeric reverse osmosis and nanofiltration membranes, J. Membr. Sci. (1996) 253-268.

[61] S.S. Deshmukh, A.E. Childress, Zeta potential of commercial RO membranes: influence of source water type and chemistry, Desalination 140 (2001) 87-95.

[62] J. P. Croué and D, A. Reckhow, Destruction of chlorination byproducts with sulphite,. Environ. Sci. Technol. 23 (1989) 1412-1419.

[63] D. A Reckhow, T. L. Platt, A.L.MacNeill, J.N. McClellan, Formation and degradation of dichloroacetonitrile in drinking waters, J. Water Supply Res. T. 50 (2001) 1-13.

[64] T. I. Bieber, M. L. Trehy, Dihaloacetonitriles in chlorinated natural waters. Ann Arbor, MI, Ann Arbor Science Publisher (1983).

[65] A. D., Nikolaou, T. D. Lekkas, M.N. Kostopoulou, S.K. Golfinopoulos, Investigation of the behaviour of haloketones in water samples, Chemosphere 44 (2001) 907-912.

[66] D. A. Reckhow, P. C. Singer, Mechanisms of Organic Halide Formation During Fulvic Acid Chlorination and Implications with Respect to Pre-ozonation. Chelsea, Lewis Publishers (1985).

[67] W. Mabey, T. Mill Critical review of hydrolysis of organic compounds in water under environmental conditions, J Phy Chem Ref Data 7 (1978) 383-416.

Highlights:

- Similar rejection behaviour within DBP groups in varying operational conditions
- Temperature had the greatest impact followed by transmembrane flux
- Using a large data set a model was developed and validated
- A different DBP group could be modelled in a range of operational conditions